

Are GRB 980425 and GRB 031203 real outliers or twins of GRB 060218?

G. Ghisellini¹, G. Ghirlanda¹, S. Mereghetti², Z. Bosnjak¹,
F. Tavecchio¹ and C. Firmani^{1,3}

¹ *INAF, Osservatorio Astronomico di Brera, via E. Bianchi 46, I-23807 Merate (LC), Italy*

² *INAF, IASF–Milano, via Bassini 15, I-20133 Milano, Italy*

³ *Instituto de Astronomía, U.N.A.M., A.P. 70-264, 04510, México, D.F., México*

5 February 2008

ABSTRACT

GRB 980425 and GRB 031203 are apparently two outliers with respect to the correlation between the isotropic equivalent energy E_{iso} emitted in the prompt radiation phase and the peak frequency E_{peak} of the spectrum in a νF_{ν} representation (the so-called Amati relation). We discuss if these two bursts are really different from the others or if their location in the $E_{\text{iso}}-E_{\text{peak}}$ plane is the result of other effects, such as viewing them off-axis, or through a scattering screen, or a misinterpretation of their spectral properties. The latter case seems particularly interesting after GRB 060218, that, unlike GRB 031203 and GRB 980425, had a prompt emission detected both in hard and soft X-rays which lasted ~ 2800 seconds. This allowed to determine its E_{peak} and total emitted energy. Although it shares with GRB 031203 the total energetics, it is not an outlier with respect to the Amati correlation. We then investigate if a hard-to-soft spectral evolution in GRB 031203 and GRB 980425, consistent with all the observed properties, can give rise to a time integrated spectrum with an E_{peak} consistent with the Amati relation.

Key words: gamma-ray: bursts — radiation mechanisms: non-thermal — scattering — X-rays: general

1 INTRODUCTION

Amati et al. (2001) found a correlation between the energy emitted (assuming isotropy) during the prompt phase of Gamma-Ray Bursts (GRBs), E_{iso} , and the frequency where most of this energy is emitted, E_{peak} (the so called Amati relation). Later, Ghirlanda, Ghisellini & Lazzati (2004) found a much tighter correlation between E_{peak} and the collimation corrected energy E_{γ} , for those bursts of known jet semi-aperture angle θ_j (the so called Ghirlanda relation). These authors also showed that all but two bursts of known redshift and E_{peak} are consistent with the Amati relation. This was confirmed more recently by Ghirlanda et al. (2005, see also Bosnjak et al. 2006) with a large sample of BATSE bursts with pseudo-redshifts (taken from Band, Norris & Bonnell 2004), despite some claims of the opposite (Nakar & Piran 2005; Band & Preece 2005). The two *outliers* with respect to the Amati relation (and also with respect to the Ghirlanda relation) are GRB 980425 and GRB 031203. Both of them are associated with an observed supernova of type Ic, i.e. GRB 980425–SN 1998bw (Galama et al. 1998) and GRB 031203–SN 2003lw (Malesani et al. 2004, Thomsen et al. 2004), but also GRB 030329 (i.e. Stanek et al. 2003),

GRB 021211 (Della Valle et al. 2002) and the very recent GRB 060218 (Campana et al. 2006; Pian et al. 2006) are associated with a SN. Unlike GRB 980425 and GRB 031203, the other bursts so far associated with a supernova event obey the Amati relation. The two outliers are very close to Earth, with a redshift of $z = 0.0085$ (GRB 980425, Tinney et al. 1998) and $z = 0.106$ (GRB 031203, Prochaska et al. 2004). Interestingly, GRB 060218 has an intermediate redshift $z = 0.033$ (Mirabal & Halpern 2006; Masetti et al. 2006), therefore it is a factor ~ 3 more distant than GRB 980425 and a factor ~ 3 closer than GRB 031203. Note that the other two GRBs associated with a supernova have $z = 0.168$ (GRB 030329, Greiner et al. 2003) and $z = 1.01$ (GRB 021211, Vreeswijk et al., 2002).

The aim of this paper is to discuss if these two bursts are real or only *apparent* outliers. We will explore three different possibilities:

- (i) these two GRBs are seen off axis, as proposed by Ramirez–Ruiz et al. (2005);
- (ii) what we see is the radiation surviving after having crossed a Thomson scattering screen;
- (iii) the real prompt emission of these bursts is subject to

a relatively strong hard to soft spectral evolution, and what we have seen is only the hardest, short-duration part of a much longer emission.

Possibility i) is quite popular, and postulates that the two outliers are normal GRBs observed off axis, at a viewing angle θ_v of the order of twice the aperture angle of the jet θ_j . (Ramírez-Ruiz et al. 2005; see also other off-axis models by Yamazaki, Ionetoku & Nakamura, 2004; Eichler & Levinson 2004) The appeal of this idea is that, within the homogeneous jet scenario, such outliers *must* exist, and should outnumber “normal” GRBs by a large factor, given by the solid angle ratios. Of course, since the received radiation for off-axis observers is strongly dimmed by de-beaming, the actual number of observable outliers depends on an accurate calculation of how both the peak energy and the total time integrated flux depend on the viewing angle θ_v , the jet aperture θ_j and the bulk Lorentz factor Γ .

Possibility ii) postulates the existence of some scattering material along the line of sight, following the original idea of Brainerd (1994) and Brainerd et al. (1998), and later used also by Barbiellini et al. (2004). In this case we are receiving the transmitted flux piercing through the scattering screen. The received flux can be much dimmer than the incident one, and the energy decline of the (Klein–Nishina) scattering cross section imprints an important modification on the transmitted spectrum making it harder and peaking at a larger E_{peak} . The intrinsic spectrum of the two outliers is then softer and brighter, and thus possibly consistent with the Amati relation.

Case iii) is based on spectral evolution. For GRB 031203, in fact, there is a strong observational evidence that what INTEGRAL has seen is only a part of a more complex story: besides the high energy emission above 20 keV, observed to have a flat spectrum and lasting for ~ 30 seconds, there must be a significant emission at much softer energies, lasting for much longer (i.e. more than a few hundred seconds, see section 4). This has been inferred through the X-ray flux scattered by dust layers in our Galaxy and producing time variable expanding rings around the source (Vaughan et al. 2004). The fluence of this component may have exceeded the fluence above 20 keV, and this supports the idea that it belongs to the prompt emission. The peak frequency of the combined soft and hard components, albeit uncertain, could well be in the range 3–10 keV, making GRB 031203 consistent with the Amati relation. In exploring this idea, we find strong similarities (and some differences) with the behaviour of a recent bursts, observed by SWIFT, namely GRB 060218. Its prompt emission lasted for ~ 3000 seconds, enabling the XRT instruments to follow most of it: for this burst we then have direct information of the high and low energy spectral components. Spectral fitting of the combined (XRT+BAT) spectra yields a peak frequency perfectly consistent with the Amati relation. Since its bolometric isotropic emitted energy is almost the same of GRB 031203, it is natural to consider them as twins.

Then the question: is it possible that even GRB 980425 had a similar behaviour? Is it possible that the prompt emission as observed by BATSE on one hand, and by the WFC and GRBM instruments of *BeppoSAX* on the other, was only part of a more complex story, and that the time in-

tegrated E_{peak} is much smaller than what measured in the first ~ 50 seconds?

To determine if the two outliers are really so or they only *appear* as such, is important for several reasons.

For instance, Paczynski & Haensel (2005) recently proposed that all “classical” GRBs are associated to the transition from a neutron to a quark star. The two outliers, in this framework, should correspond to massive stars outgoing the SN Ic explosion *without* undergoing the transition to the quark star. Clearly, in this view, GRB 980425 and GRB 031203 are real outliers, emitting their prompt radiation with different mechanisms than the other, “classical” GRBs. Moreover, if these two bursts are real outliers they should have a flatter luminosity function with respect to “normal” GRBs in order to account for their lower detection rate, as recently discussed by Liang, Zhang and Dai (2006).

On the contrary, if the two GRBs are not outliers, than we strengthen the Amati relation, which becomes more universal. Its physical interpretation therefore becomes even more compelling.

2 HOMOGENEOUS JET SEEN OFF AXIS

Assume that the radiation is collimated into a cone of semi-aperture angle θ_j and that the angle between the jet axis and the line of sight is θ_v . The fireball emits, in its comoving frame, a time integrated spectrum described by a double power law, smoothly joining at some frequency ν'_c . This function is a simplified version of the popular Band model (Band et al. 1993) composed by two powerlaws smoothly joined by an exponential cutoff. Calling $x' \equiv \nu'/\nu'_c$, the time integrated energy spectrum, $\mathcal{E}'(x')$, is

$$\mathcal{E}'(x') = k \frac{x'^{-\alpha_1}}{1 + x'^{\alpha_2 - \alpha_1}} \quad (1)$$

where α_1 and α_2 represent the power laws' energy indices below and above ν'_c , respectively. Since the velocity vectors of the fireball are radially distributed within θ_j , we need to integrate, with the appropriate beaming factor, over the entire fireball surface in order to derive the energy spectrum observed at θ_v . Calling $\delta \equiv [\Gamma(1 - \beta \cos \theta)]^{-1}$ we have

$$E(x, \theta_v) = \int_{\max(0, \theta_v - \theta_j)}^{\theta_v + \theta_j} \Delta\psi \delta^2 \mathcal{E}'(x/\delta) \sin \theta d\theta \quad (2)$$

Within the limits of integration, the factor $\Delta\psi$ is given by (see Ghisellini & Lazzati 1999)

$$\begin{aligned} \Delta\psi &= 2\pi; & \theta < \theta_j - \theta_v \\ \Delta\psi &= \pi + 2 \arcsin \left(\frac{\theta_j^2 - \theta_v^2 - \theta^2}{2\theta\theta_v} \right); & \theta \geq \theta_j - \theta_v \end{aligned} \quad (3)$$

We then define $E_{\text{peak}}(\theta_v)$ as the maximum of the $x E(x, \theta_v)$ function. In Fig. 1 we plot E_{peak} as a function of the time integrated flux $E(\theta_v) = \int E(x, \theta_v) dx$, having assumed $\theta_j = 5^\circ$, and varying θ_v between 0° and 20° . The three curves correspond to $\Gamma = 50, 100$ and 200 . It can be seen that the $E_{\text{peak}} \propto E^{1/3}$ behaviour (dotted line in Fig. 1) is reached only for large viewing angles. In the insert, the zoom for small viewing angles shows that E changes by a factor 2 for $0 < \theta_v < \theta_j$, while E_{peak} remains approximately constant.

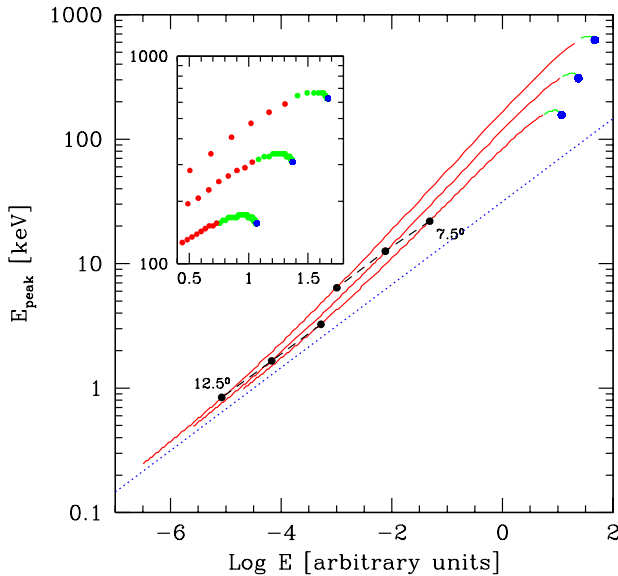


Figure 1. The peak of the observed spectrum E_{peak} as a function of the time integrated flux E . Both depend on the viewing angle θ_v . In the insert we show a zoom for small viewing angles, within (green dots) and outside θ_j . We assumed $\theta_j = 5^\circ$, $0 < \theta_v < 20^\circ$, $\alpha_1 = 0.5$, $\alpha_2 = 2$. The dotted line, shown for comparison, has a $1/3$ slope. The three lines have $\Gamma = 50, 100$ and 200 , and $E'_{\text{peak}} = 1.25$ keV. Black points, connected with dashed lines, correspond to the same viewing angle $\theta_v = (7.5, 12.5)$ for the three different choices of Γ .

The reason for the departure from the $E_{\text{peak}} \propto E^{1/3}$ behaviour is the following (see also Eichler & Levinson 2004 and Toma et al. 2005): for large viewing angles, there is a small difference between the flux received from the near and the far edges of the jet, which therefore contribute equally to the total flux. As long as this is the case, we have $E_{\text{peak}} \propto E^{1/3}$. As the viewing angle is decreased, the difference of the fluxes received from the edges increases, with the far edge becoming progressively negligible (with respect to the near edge), causing a deficit of total flux with respect to the extrapolation from larger viewing angles.

The reason of the factor 2 difference between the energy observed at $\theta_v = 0$ and $\theta_v = \theta_j$ is the following: on axis observers receive most of the flux from a circle of angular radius $1/\Gamma$. At the border of the jet (i.e. for $\theta_v = \theta_j$) only \sim half of the circle is inside the jet and emitting. The maximum value of E_{peak} is not observed by observers perfectly on-axis, but slightly off. To explain this effect consider the on-axis observer: in this case the maximum flux is again received by the ring of angular radius $1/\Gamma$, with contributions both from smaller angles (with larger E_{peak}) and larger angles (with smaller E_{peak}). The observed E_{peak} is found by integrating the spectra over the jet solid angle. For slightly off-axis observers, the contribution from large angles (on one side of the jet) is partially missing (lying outside the jet solid angle), while it appears a contributions from still larger angles from the opposite side of the jet. This latter component is too de-beamed to compensate for the missing one and the net effect is to slightly increase the observed E_{peak} .

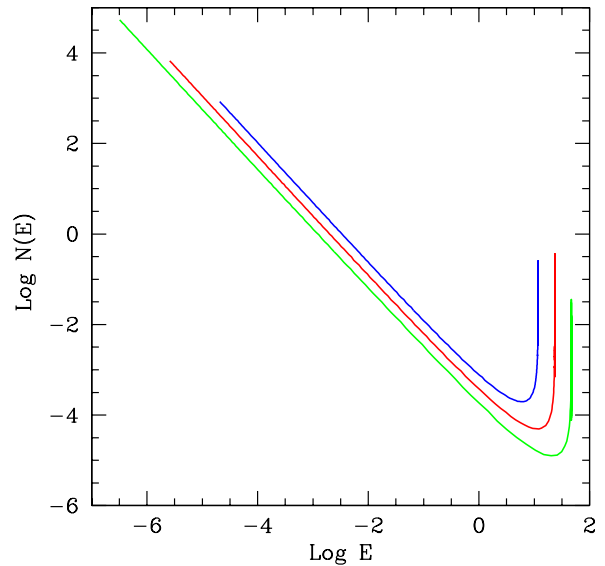


Figure 2. The “energy function” $N(E)$ (i.e. the time integrated luminosity function) for the 3 cases corresponding to $\Gamma = 50, 100$ and 200 (upper, intermediate and lower lines) shown in Fig. 1.

2.1 The “energy” function

Assume that a subset of bursts have all the same radiated energy E_{on} if seen on axis. Bursts observed off-axis will be observed to emit an energy E , and their number is proportional to the corresponding solid angle (see Urry & Shafer 1984 and Celotti et al. 1993 for blazars):

$$N(E, E_{\text{on}})dE = \frac{d\Omega}{2\pi} = \sin\theta d\theta \quad (4)$$

leading to

$$N(E, E_{\text{on}}) = \left(\frac{dE}{d\cos\theta} \right)^{-1} \quad (5)$$

If bursts have an intrinsic distribution $\Phi(E_{\text{on}})$ of energetics as seen on axis, than we have to integrate $N(E, E_{\text{on}})$ over that distribution.

Fig. 2 shows $N(E, E_{\text{on}})$ for the three cases shown in Fig. 1 (i.e. $\Gamma = 50, 100$ and 200). The resulting function is a power law at small energies, and note the increase towards the upper end of the energy range. This corresponds to observers within the jet aperture angle, who see almost the same energetics. At small energies, the slope of the power law is $4/3$. This value has a simple explanation. For large viewing angles, in fact, the observed energy $E \propto \delta^3 \propto [\Gamma(1 - \cos\theta)]^{-3}$. Therefore $(dE/d\cos\theta)^{-1} \propto \delta^{-4} \propto E^{-4/3}$, which is a very good approximation of the numerical results shown in Fig. 2¹.

2.2 Application to GRB 980425 and GRB 031203

If GRB 980425 and GRB 031203 were off-axis events and we require their on-axis energetics to satisfy the Amati relation,

¹ This results is general, as demonstrated by Urry & Shaefer (1984): for beaming amplification factors $L \propto \delta^p$, the resulting low luminosity branch of the observed luminosity function $N(L) \propto L^{-1-1/p}$.

then we end up to isotropic energies larger than 10^{53} erg (even larger than suggested by Ramirez-Ruiz et al. 2004 for GRB 031203 using a $E_{\text{iso}} \propto E_{\text{peak}}^{1/3}$ approximation).

All models invoking an intrinsic very large energy output, similar or even larger than the energy output of “classical” GRBs, suffer from a severe problem: the two outliers are the closest of all GRBs and it is therefore extremely unlikely that such energetic bursts exist in our vicinity, for all reasonable luminosity functions (or energy functions). This issue has been discussed in Guetta et al. (2004) and with the detailed “trajectories” calculated in the previous sections the problem is even worse than assuming the naive $E_{\text{peak}} \propto E_{\text{iso}}^{1/3}$ behaviour, since the steeper dependence requires larger values of E_{iso} to become consistent with the Amati relation. For this reason, we discard this possibility.

On the other side, if jets are homogeneous, we *must* observe some of them slightly off axis. For a given sensitivity threshold, the amount of them depends on the specific value of the bulk Lorentz factor Γ , since larger Γ make the received flux to decrease more rapidly increasing the viewing angle. This can be seen in Fig. 1, where we have marked the points corresponding to the same viewing angles: increasing by a factor 2 the bulk Lorentz factor implies to decrease by an order of magnitude the measured E_{iso} . Fig. 2 makes this argument more quantitative, showing the relative number of expected off-axis sources with respect to on-axis ones.

This is not meant to discard the fact that some GRBs can be seen off-axis, but only to discard the fact that this is the only reason for bringing the two outliers over the Amati relation.

3 PIERCING THROUGH A SCATTERING SCREEN

As already discussed, the vicinity of the two outliers argues against these two bursts being normal powerful bursts seen off-axis, (with, say, $E_{\text{iso}} \sim 10^{53}$ erg or more, as suggested by Ramirez-Ruiz et al. 2004) since any reasonable luminosity function would make them extremely rare in the volume corresponding to their redshifts. Instead, their vicinity argues in favour of an intrinsically small isotropic energy and luminosity (see e.g. Guetta et al. 2004). We then investigate whether these two bursts are observed through a screen of large optical depth, which at the same time decreases their apparent isotropic energy and *increases* their apparent E_{peak} . Their intrinsic emission (i.e. before passing through the scattering screen) could then be consistent with the Amati relation.

3.1 Transmitted spectra

The spectrum, incident on a screen of large optical depth, is assumed to be a smoothly joined broken power law (with energy indices α and β at low and high frequencies, respectively) as in Sec. 2, or a single power law ending with an exponential cut:

$$\begin{aligned} F(x) &= F_0 \frac{(x/x_b)^{-\alpha}}{1 + (x/x_b)^{\beta-\alpha}}; \\ F(x) &= F_0 x^{-\alpha} \exp(-x/x_c) \end{aligned} \quad (6)$$

where $x \equiv h\nu/(m_e c^2)$ is the photon energy in units of the electron rest-mass energy. We assume that $\alpha < 1$ and $\beta > 1$.

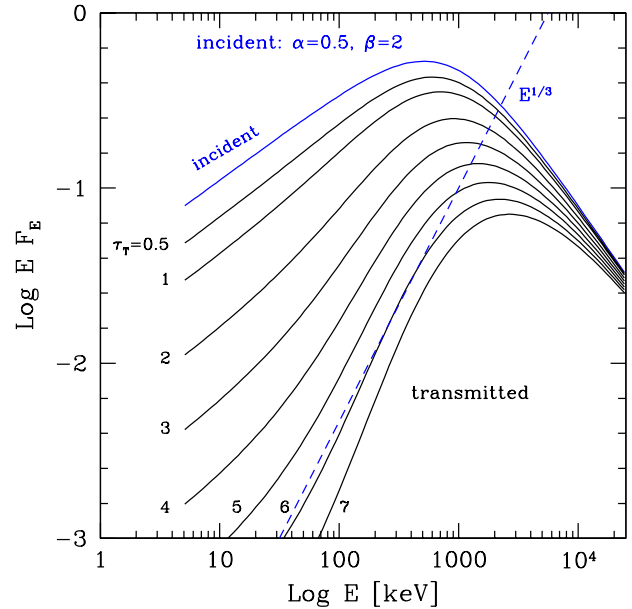


Figure 3. Transmitted spectrum for different values of the Thomson optical depth τ_T , as labelled. The incident spectrum has $E_{\text{peak}} = 511$ keV, $\alpha = 0.5$ and $\beta = 2$. The chosen value of α corresponds to the hardest synchrotron slope produced by a cooling population of electrons. The dashed line, $\propto E^{1/3}$ corresponds to the hardest possible synchrotron slope produced by an electron distribution with a low energy cut-off, and no cooling. Harder spectra are difficult to reconcile with the standard synchrotron interpretation (Ghirlanda, Celotti & Ghisellini 2003). Note that we can have transmitted spectra harder than $\alpha = -0.3$, even with incident spectra having $\alpha = 0.5$, for $\tau_T > 6$.

Thus, in a $xF(x)$ representation, the peak energy x_{peak} is $x_{\text{peak}} = x_b [(1 - \alpha)/(\beta - 1)]^{1/(\beta - \alpha)}$ for the broken power law case and $x_{\text{peak}} = x_c(1 - \alpha)$ for the cut-off power law case.

Along the line of sight the Thomson optical depth is $\tau_T = \sigma_T n \Delta R$, where n is the number density and ΔR is the typical size of the scattering region. We will consider values of τ_T even larger than one, and this is possible only if the scattering region is close to the burst, and becomes almost completely ionized by the prompt emission. Otherwise, we would detect very large column densities in the X-ray spectra of the afterglow. The Klein Nishina optical depth is $\tau_{\text{KN}} = \tau_T \sigma_{\text{KN}}/\sigma_T$. The *transmitted* luminosity is the luminosity passing through the scattering material without suffering any scattering:

$$F_t(x) = F(x) \exp(-\tau_{\text{KN}}) \quad (7)$$

Fig. 3 shows the transmitted spectra for different values of τ_T for an incident spectrum peaking at $E_{\text{peak}} = 511$ keV, with $\alpha = 0.5$ and $\beta = 2$. Incidentally, note that the assumed α corresponds to the spectrum produced by a cooling population of electrons, but with an initial low energy cutoff (see Ghisellini, Celotti & Lazzati 2000). The effect of scattering hardens the transmitted spectrum, to reach values harder than $\alpha = -1/3$ (the “line of death” for the synchrotron interpretation, Preece et al. 1998), for $\tau_T > 6$.

The other effect imprinted on the transmitted spectrum by the scattering screen is the shift of the peak en-

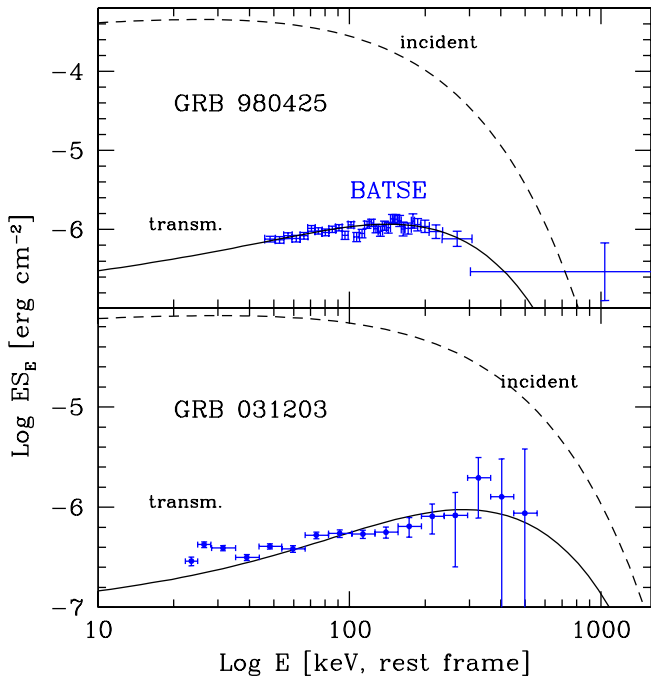


Figure 4. The observed $ES(E)$ spectra of the prompt emission of GRB 980425 (top panel) as observed by BATSE and of GRB 031203 (bottom panel) as observed by INTEGRAL, expressed in fluence units. The data shown for GRB 980425 have been analyzed by us using a power law with an exponential cut-off to fit the time integrated spectrum over the ~ 30 sec duration of the burst. For GRB 031203, we report the spectrum analyzed by us, using version 5.1 of the OSA analysis software and the corresponding response matrices. This spectrum corresponds to the first 20 sec of the emission as the following 20 to 40 sec do not contribute significantly. Solid lines corresponds to the flux passing through a screen of material, while dashed lines are the intrinsic flux (i.e. before passing through the screen). The parameters of the model are listed in Table 1.

ergy E_{peak} to higher values, as shown in Fig. 3. This is due to the declining (with energy) Klein–Nishina cross section σ_{KN} . For instance, the transmitted spectrum in the case of $\tau_{\text{T}} = 6$ has $E_{\text{peak}} \sim 2$ MeV, while the intrinsic spectrum has $E_{\text{peak}} = 511$ keV.

Note also that the bolometric transmitted energy, for this particular case of an intrinsic $E_{\text{peak}} = 511$ keV, decreases much less than the factor $\exp(-\tau_{\text{T}})$ expected in the Thomson regime (a factor ~ 10 for $\tau_{\text{T}} = 5$, instead of the factor 150 we would have in the Thomson regime).

3.2 Application to GRB 980425 and GRB 031203

In Fig. 4 we show the observed spectrum of the two sources (time integrated over the duration of the bursts), the assumed intrinsic spectrum, and the transmitted one.

We reanalyzed the INTEGRAL data obtained with the IBIS/ISGRI instrument using version 5.1 of the OSA analysis software and the corresponding response matrices. The spectrum corresponding to the first 20 seconds of the burst (start time 2003–12–03 22:01:26) can be fit by a power law with photon index 1.7 and fluence 1.4×10^{-6} erg cm^{-2} .

The found slope is consistent with the slope found by

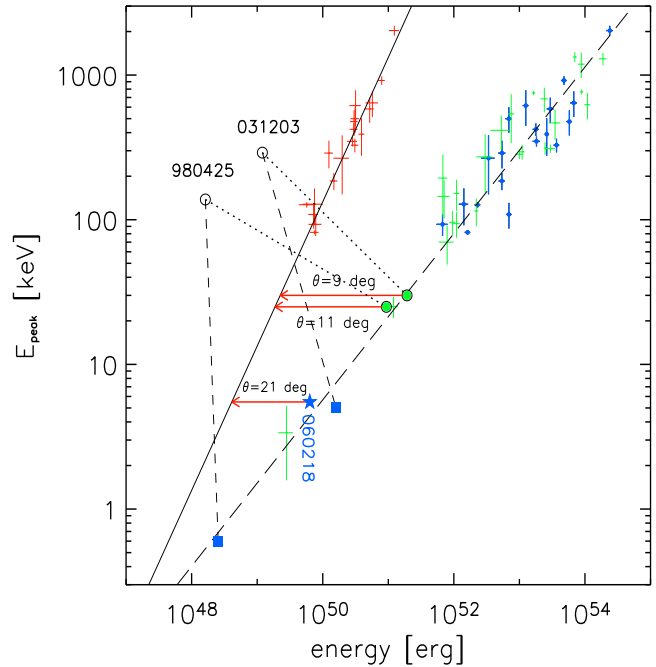


Figure 5. The correlation between E_{peak} and the isotropic equivalent energy radiated during the prompt emission E_{iso} (blue and green symbols, the “Amati” relation, Amati et al. 2002)) and the collimation corrected energy $E_{\gamma} = (1 - \cos \theta_j) E_{\text{iso}}$, where θ_j is the semiaperture angle of the jet, assumed conical (red crosses, the “Ghirlanda” relation, Ghirlanda et al. 2004, but here shown in the case of a circumburst density profile $n \propto r^{-2}$ appropriate for a stellar wind made by the progenitor, see Nava et al. 2006). Blue points are the 19 GRBs with a firm estimate of the jet opening angle; green points are those bursts (adapted from Amati et al. 2006) without a firm estimate of θ_j . GRB 980425 and GRB 031203 are outliers (open circles) with respect to the “Amati” relation (long-dashed line), but they can be made consistent with this correlation dotted line and green filled circles) by assuming that the radiation we see is the transmitted radiation crossing a scattering screen as illustrated in Fig. 4. Without the scattering screen, these two bursts would have appeared as intermediate between X-ray rich GRB and X-ray flashes. Moreover, they can be made consistent with the Ghirlanda relation (solid line, in the case of a “wind” density profile) if their jet opening angle is 9° and 11° , as labelled. GRB 060218 would be consistent with the Ghirlanda relation for $\theta_j \sim 21^\circ$. Alternatively we also show the effect of spectral evolution (Sec. 4) which can make the two outliers consistent with the “Amati” relation (short-dashed line and blue-filled squares) if we only detected a short portion of their much longer emission which rapidly evolved from the hard γ -ray band to the soft X-ray band. In this case, if we require that these two bursts are consistent with the “Ghirlanda” relation we derive angles of 34° and 13° for GRB 980425 and GRB 031203, respectively.

Sazonov et al. (2004), but smaller by a factor 1.4 in normalisation.

For GRB 980425 we have analysed the BATSE data (to show the data points) using a cut-off power law model. The best fit parameters are $\alpha = 0.45 \pm 0.22$ and $E_{\text{peak}} \sim 138$ keV ($\chi^2 = 109/97$ dof), giving a flux of $\sim 10^{-7}$ erg/ cm^2 sec (40–700 keV), consistent with that reported in Pian et al. 2000.

The same model (power law + exponential cut) was

GRB	τ_T	α	E_c	$E_{\text{peak}}^{\text{intr}}$ keV	$E_{\text{peak}}^{\text{obs}}$ keV	θ_j	f
980425	7.5	0.7	83.3	25	138	11°	577
031203	6.5	0.85	200	30	292	9°	161

Table 1. Input parameters of the scattering model for the two outliers. The parameter f is the ratio of the intrinsic to transmitted total energy. The jet opening angle θ_j is derived requiring that the the intrinsic E_{peak} and E_γ fit the “Ghirlanda” relation derived under the wind circum-burst density hypothesis (Nava et al. 2006).

assumed for GRB 031203, for which we plot the spectrum analyzed by us in Fig. 4, but with frequencies in the source rest frame. For GRB 031203 a soft component has been inferred through the observed transient rings produced by the scattering of the burst radiation by dust layers in our own Galaxy (Vaughan et al. 2004, Tiengo & Mereghetti 2006 – see also Vaughan et al. 2006 for another case of dust scattering halo associated with GRB 050724). This component, that will be discussed in the next section, is here neglected.

It can be seen in Fig. 4 that the model can reproduce the observed data quite satisfactorily. In Tab. 1 we report the assumed parameters (τ_T , α , E_c) for GRB 980425 and GRB 031203, and in Fig. 5 we show where these two bursts “move” in the $E_{\text{peak}}-E_{\text{iso}}$ plane (filled circles) when the incident spectrum (i.e. that impinging on the scattering screen) is reconstructed with the assumed parameters. In Fig. 5 we also show what jet opening angle θ_j they should have to also fit the “Ghirlanda” relation between E_{peak} and the collimation corrected energy $E_\gamma = (1 - \cos \theta_j)E_{\text{iso}}$, as derived under the hypothesis of a wind density environment (Nava et al. 2006). This angle turns out to be $\sim 9^\circ$ for GRB 031203 and $\sim 11^\circ$ for GRB 980425. These values of θ_j lie in the large-angle tail of the distribution of known jet opening angles (for 19 GRBs – see Fig. 6 in Nava et al 2006). In fact, the low peak energies of the intrinsic spectra (i.e. before piercing through the scattering screen) places both GRB 980425 and GRB 031203 in the XRF region of the $E_{\text{peak}}-E$ plane of Fig. 5 where the “Amati” and “Ghirlanda” correlation converge. Bursts in this region have, on average, jet opening angles larger than those placed at the opposite extreme (such as e.g. GRB 990123, the most energetic burst in the $E_{\text{peak}}-E_{\text{iso}}$ and in the $E_{\text{peak}}-E_\gamma$ planes).

Although this “screen model” might have interesting feature, it suffers from some problems, related to the presence of an optically thick screen itself. The first problem is why this material is present in some bursts but not in others. An additional problem concerns its location: if it is at some distance from the bursts, its material would not be ionized (and the dust in it not destroyed) by the prompt radiation, making the optical afterglow not detectable. If it is instead located close to the burst, one should see some signature of its presence when the fireball and/or the supernova ejecta collide with it.

4 SPECTRAL EVOLUTION

The scenarios presented in the previous sections were aimed to explain the prompt emission as observed by BATSE and

BeppoSAX for GRB 980425, and by INTEGRAL for GRB 031203, assuming that the received prompt emission was mainly in the 20–300 keV range. This may not be true, however, for the following reasons:

- The echo-rings detected by XMM-Newton a few hours after the trigger of GRB 031203 can be produced only if the incident flux is at soft X-ray energies and large. Reconstructing the flux, fluence and spectrum of the emission which was scattered by the dust layers of our Galaxy is not straightforward, but the existing estimates point towards a total fluence at least as large as the fluence detected by INTEGRAL, at energies around 1 keV (Watson et al. 2006; Tiengo & Mereghetti 2006). In this respect, note that the re-analysis of the INTEGRAL data performed by us, with improved detector response matrices yields a total fluence a factor 1.4 less than what quoted by Sazonov et al. (2004), while the spectral shape is the same.

- One important issue is if this soft component belongs to the prompt emission or if it is instead the beginning of the afterglow. The large fluence, however, suggests that this is part of the prompt, since we never observed X-ray afterglows as bright as the prompt in any other GRB.

- Another issue concerns the duration of the soft component. A lower limit can be roughly estimated based on the the lack of detection with IBIS/ISGRI in the images obtained after (and before) the GRB prompt emission. Such images are limited to the energy range above ~ 17 keV. Therefore one has to invoke either that the soft X-ray emission desumed from the dust scattering rings had a spectrum with a very sharp cut-off before the IBIS/ISGRI energy range or that the soft X-ray emission lasted more than several hundred seconds, in order to give the required fluence without violating the flux upper limits. Note that a duration of the order of a few thousand seconds would still be compatible with the observed width of the expanding rings measured with XMM-Newton.

- For GRB 980425 we do not have direct evidences of the presence of a (possibly long-lasting) soft component, but we do have some indication of spectral softening from the analysis of the WFC (Wide Field Camera) and GRBM monitor on board *BeppoSAX*, as presented by Frontera et al. (2000), see the spectra reported in Fig. 9. The total fluence in the WFC [2–28 keV] is of the same order than the fluence in GRBM (which agrees with BATSE).

- The idea of an hard-to-soft spectral evolution, with a very long soft emission, received a strong support from the recently *Swift* GRB 060218 (Cusumano et al. 2006). For this burst the narrow field instruments of Swift could follow the emission for most of the prompt phase, which lasted at least ~ 3000 seconds (Barthelmy et al. 2006). This burst showed a hard-to-soft spectral evolution, and its time integrated spectrum has a peak energy around 5 keV and a $\sim 6 \times 10^{49}$ erg isotropic energy which makes this burst fully consistent with the Amati relation (Campana et al. 2006; see Fig. 5). The total energetics of GRB 060218 is very similar to the one of GRB 031203, and both are associated with a supernova of similar power (e.g. Cobb et al. 2006). This burst prompted us to explore in some detail the idea of spectral evolution for the two outliers.

- Finally we point out that, recently, a tight correlation was discovered (Firmani et al. 2006), involving only observ-

ables belonging to the prompt emission: the peak luminosity, E_{peak} and the “high signal” timescale $T_{0.45}$ (it is the same timescale used for the characterization of variability, see Reichart et al. 2001). GRB 980425 and GRB 031203 are outliers with respect to this correlation. However GRB 031203 would become consistent with this newly found correlation if E_{peak} were in the $\sim\text{keV}$ range, as suggested by the echo-rings.

In this section we see if it is possible to construct a simple model for the spectral evolution of GRB 031203 and GRB 980425 that is at the same time consistent with the existing observations of these two GRBs and also predicting, for their time integrated spectra, values of E_{peak} and E_{iso} in agreement with the Amati relation. We are inspired to do such a modelling by the behaviour of GRB 060218, and we will then first construct our toy model in order to reproduce the time-dependent behaviour of its spectra. For this burst we have much more information than for the others, and the modelling therefore merely implies to characterise the spectral index, the cut-off energy and the normalisation of the spectrum with smooth functions of time, to reconstruct both the time resolved spectra and the light curves in the XRT [0.3–10 keV] and BAT [15–150 keV] energy bands.

For GRB 031203 the time dependent information is almost not existent: we assume that the soft X-ray spectrum and fluence, around 1 keV, is the one inferred (albeit in an approximate way), by the echo-rings observed by XMM-Newton.

For GRB 980425 we have even less information, and the modelling is done only to show that there is no evidence against a hard-to-soft evolution also for this burst.

We are aware that i) this model does not pretend to be unique, since it can be one of many spectral evolution models; ii) it is completely phenomenological, and it has no theoretical support, iii) for the sake of simplicity, we will assume that the spectral indices and the high energy cut off of the spectrum, as well as its normalisation, are smooth functions of time (i.e. we will assume no flares), and finally iv) even if we will minimise the number of free parameters, in the end we need many.

These can be taken as strong limitations if we were really seeking “the” model for interpreting the properties of spectral evolution, but this is not our aim. Our goal is instead to demonstrate that, even with a naive and simple approach, it is indeed possible to fulfil the two requirements of being in agreement with all observations and nevertheless making these specific bursts to obey the Amati relation.

4.1 The case of GRB 060218

Fig. 6 (upper panel) shows the time integrated spectrum of GRB 060218. We re-analyzed the XRT data of the first ~ 2600 sec (in *wt* mode) starting ~ 159 sec after the BAT trigger (03:34:30 UT - Cusumano et al. 2006). For the data extraction we used the standard *xrtpipeline* (v.0.9.9) and for the spectral analysis we used the v.007 detector response matrix (for *wt* mode limited to grades 0–2). Campana et al. 2006, through a joint XRT–BAT fit, found that the peak energy $E_{\text{peak}} \sim 4.5$ keV lies in the XRT energy range, and the spectrum can be fitted by the sum of a black-body (BB) and a cut-off power law (CPL). We show in Fig. 6 the X-ray data as re-analysed by us, together with the best fit model

(dashed lines). The duration of this burst was so long that the BAT “burst” mode data contained only the first ~ 350 sec of its emission. The study of the following portion of the burst requires the analysis of the “survey” mode data which are more difficult to handle, we believe that the BAT team can analyse these data more appropriately than us. However, the BAT team already gives the total BAT fluence for this burst (Campana et al. 2006). We have then fitted the XRT time integrated spectrum with the same model (i.e. BB+CPL and same $N_{\text{H}} = 6 \times 10^{21} \text{ cm}^{-2}$ – see Campana et al. 2006), using the BAT fluence (Campana, priv. comm.; Dai, Zhang & Liang 2006) as a constrain. In this way we have obtained the same E_{peak} and 0.3–10 keV fluence of Campana et al. (2006).

Through this “BAT-fluence-constrained” fit procedure we analyzed the XRT data in the same time intervals reported in Campana et al. (2006). Fig. 6 shows three spectra: the top one is the spectrum integrated over the total observed duration of the bursts, while the other two spectra correspond to the [159–309 s] and [2456–2748 s] time bins. These are the first and the last spectra that can be obtained with both XRT and BAT data, according to the time binning chosen by Campana et al. (2006), which can be also seen in the right bottom panel of Fig. 6. For the [159–309 s] time-bin the BAT “burst” mode data were available and we can then show the corresponding XRT+BAT data. For the [2456–2748 s] time-bin we only show the XRT data, fitted with the same model and procedure (i.e. forcing the fit to have the same BAT fluence reported in Campana et al. 2006) as for the time-integrated spectrum.

Note also that for all the three spectra (first and last time bin and time integrated) we show the BB component resulting from the fit (dotted lines). This component contributes at least 20% to the total spectral fluence, and it has been interpreted as due to the jet shock breakout (Campana et al. 2006). For this, we will not consider it in our spectral-evolution model.

In the right bottom panel of Fig. 6 we show the light curves in the BAT and XRT energy ranges and also the evolution of E_c (i.e. $E_c = E_{\text{peak}}/(1 - \alpha)$, where α is the energy spectral index of the CPL model). The values of E_c have been derived with the same procedure discussed above.

To model the time evolution of this burst we need the normalisation K and the spectral index α of the power law, and the cut-off energy E_c , as a function of time. For the latter we have simply interpolated the derived values with a smooth function (the combination of a very weakly rising and a decaying power law of time: solid line in the right bottom panel of Fig. 6), while the assumed behaviour of K and α are shown in the left bottom panel of the same figure. We have chosen functions which are either constants or power laws of time.

Having reconstructed in this way the entire time evolution of this burst, we could then sum-up the instantaneous spectra to give the spectra integrated in specific time bins and the spectrum integrated over the entire burst duration. Note that the time integrated spectra *are not necessarily described by a BB+CPL model, since the spectral parameters evolve*. This can be the reason why, quite often, one obtains a better fit with a time resolved spectrum rather than with a time integrated one.

The agreement with the observation is excellent, but

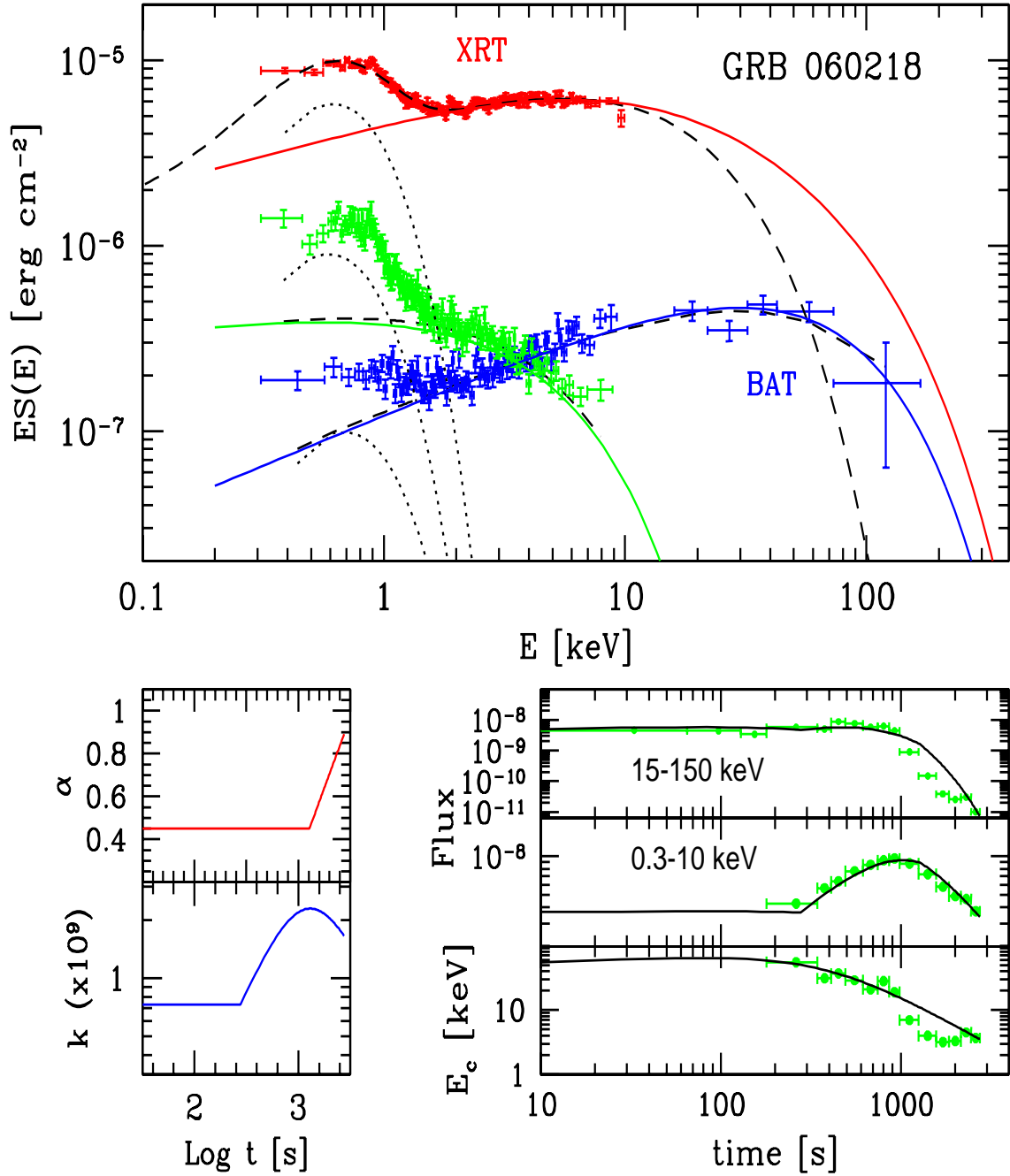


Figure 6. Top panel: Spectra of GRB 060218 for different time-bins: i) entire duration (top); ii) [159–309 s] (rising spectrum with also BAT data) iii) [2456–2748 s] (soft spectrum). We plot $ES(E)$ vs E , $S(E)$ being the fluence. Dotted lines indicate the blackbody component, not considered for the spectral evolution, and long-dashed lines represents the best fit obtained from the analysis of the data. Continuous lines show the results of our proposed modelling. Left bottom panel: assumed behaviour of the normalisation K and energy spectral index α . Right bottom panel: light curves in the BAT (15–150 keV) and XRT (0.3–10 keV) range, and evolution of E_c . The flux in the 0.3–10 keV is the (de-absorbed) flux of the cut-off power law component only: we have subtracted the blackbody component from the total flux. Continuous lines are the results of our modelling.

expected, since what we have done is merely to interpolate with smooth functions of time the real evolution of the spectral parameters. The overprediction of the flux at high energies in the time integrated spectrum (solid-red line in top panel) is due to the fact that the smooth function inter-

polating E_c lies above the data points in the second part of the time evolution (see the right bottom panel of Fig. 6).

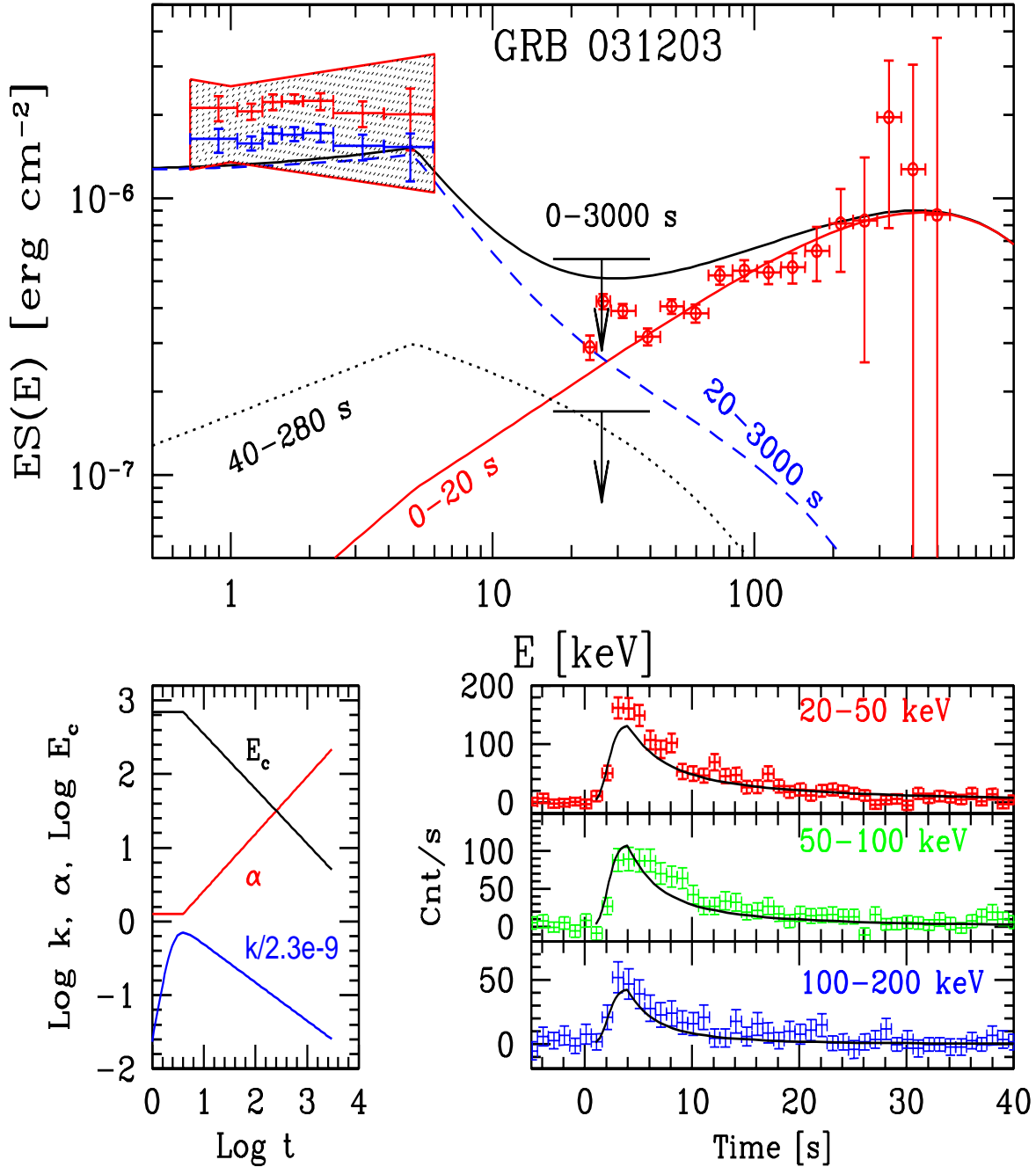


Figure 7. Top panel: the spectral energy distribution of GRB 031203 is compared with the result of our model. Here we show the INTEGRAL data as analysed by us and the low energy emission as inferred by the light scattering echo calculated by Watson et al. (2006). The bow-tie corresponds to the uncertainty in the amount of the scattering material. In addition to those, there are additional uncertainties connected to which cross section is used, as discussed in Tiengo & Mereghetti (2006). The lines corresponds to the emission time integrated in different energy intervals, as labelled. The bottom left panel shows how the normalisation $K(t)$, the high energy spectral index α and the cut-off energy E_c change in time. The right bottom panel compares the observed and the calculated light curves in the three labelled energy bands.

4.2 GRB 031203

This burst was discovered by INTEGRAL, and the spectrum in the 20–400 keV band is shown in Fig. 7. In this figure we show the spectrum as reanalysed by us (see. Section 3.2).

The soft X-ray spectrum is inferred by the light scattering echo discovered by XMM-Newton (Watson et al. 2004) and modelled by Watson et al. (2006) to get the intrinsic spectrum illuminating the galactic dust clouds. Note that Tiengo & Mereghetti (2006) re-derived the illuminating

spectrum and fluence by adopting a different cross section for the scattering process between X-ray photons and dust, obtaining a fluence somewhat smaller than Watson et al. (2006), but with a similar spectrum. Therefore both groups agree that the soft (less than a few keV) X-ray emission lies much above the extrapolation from the high energy spectrum, and that the slope of the spectrum below a few keV is softer than the 20–200 keV slope.

The lightcurves (in counts per second) in three different energy bands have been extracted by us using the most recent version of the response matrix.

The modelling of the spectral evolution of this burst is aimed to reproduce: i) the time integrated spectrum as seen by INTEGRAL in the 20–200 keV band; ii) the upper limit in the medium energy band [17–40 keV]; iii) the soft X-ray emission as inferred by the light scattering echo and iv) the light curves (in counts per second) in three different energy bands of INTEGRAL [20–50 keV; 50–100 keV and 100–200 keV].

4.2.1 Modelling the spectral evolution

We model the spectral evolution of the prompt emission assuming that the spectrum, at any time, is a broken power law ending with an exponential cut. We assume a broken power law (instead of a single one) to limit the total energetics to a finite value. For simplicity, we assume that the energy spectral index α of the low energy branch is equal to $1/2$ the value of the energy spectral index of the high energy part (we do this just to limit the number of free parameters). The two power laws connect at the break energy E_b . We assume that the cut-off energy E_c , the break energy E_b , the power law index α and the normalisation can evolve in time. We set

$$F(E, t) = K(t) \left(\frac{E}{E_b} \right)^{-\alpha(t)/2}; \quad E \leq E_b$$

$$F(E, t) = K(t) \left(\frac{E}{E_b} \right)^{-\alpha(t)} \times \exp \left[-\frac{E - E_b}{E_c(t)} \right]; \quad E \geq E_b \quad (8)$$

where the normalisation K is

$$K(t) = \frac{(t/t_m)^{b_1}}{1 + (t/t_m)^{b_1+b_2}} \quad (9)$$

here b_1 and b_2 are indices describing the evolution of the normalisation of the spectrum, and t_m is related to the time t_{\max} of the maximum of $K(t)$ by

$$t_{\max} = t_m \left(\frac{b_1}{b_2} \right)^{1/(b_1+b_2)} \quad (10)$$

The spectral index α and the cut-off energy, E_c , are assumed to evolve as power laws of time (i.e. $\alpha \propto t^a$, $E_c \propto t^{-c}$, but we allow for the possibility that they remain initially constant (for a time equal or shorter than t_{\max}). All these choices are arbitrary, the only guiding line is simplicity.

The constant K is chosen to match the observed spectral shape of the fluence the burst obtained by the high energy data.

To reconstruct the light curves in one band $\Delta E = E_2 - E_1$ keV in counts s^{-1} we multiply $F(E, t)$ by the normalised effective area $A(E)$ of the INTEGRAL instruments to get

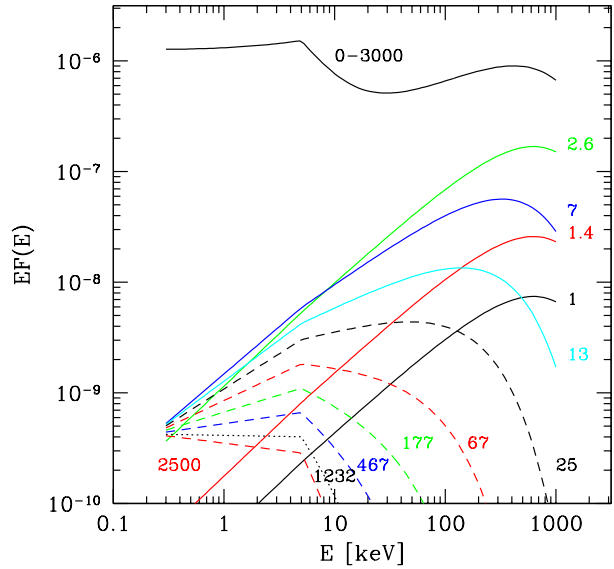


Figure 8. Calculated spectra of GRB 031203 at different times, as labelled (number are seconds). Also shown is the time integrated spectrum (time interval 0–3000 seconds).

$$C(\Delta E, t) = \int_{E_1}^{E_2} \frac{F(E, t)}{E} A(E) dE \quad (11)$$

Then we re-normalise all the light curves obtained in different energy bands by the same normalisation factor.

4.2.2 Results for GRB 031203

The left bottom panel of Fig. 7 shows the behaviour of $K(t)$, $\alpha(t)$ and the cutoff energy $E_c(t)$ which we have assumed for the spectral evolution of GRB 031203.

The top panel of Fig. 7 shows the SED resulting from our modelling, while the right bottom panel of the same figure reports the light curves of the model (solid lines) in different bands and compares those with the data. The assumed overall duration of the prompt emission is 3000 seconds: of those, only the first ~ 50 seconds have been detectable by INTEGRAL in the 20–200 keV energy band.

We can see that the assumed hard-to-soft spectral evolution is in agreement with all the information we have about the prompt emission of this burst, and predicts a peak energy of the overall spectrum at $E_{\text{peak}} \sim 5$ keV. Also the total energetics is enhanced if we include the soft X-ray prompt emission. This is shown in Fig. 5, where one can see how GRB 031203 “moves” in the $E_{\text{iso}}-E_{\text{peak}}$ plane. With the derived values of these parameters GRB 031203 obeys the Amati relation.

4.3 GRB 980425

The prompt emission of this burst was detected both by BATSE and by *BeppoSAX*. The latter detected it both with the Gamma Ray Burst Monitor (GRBM) and the Wide Field Camera (WFC) (e.g. Pian et al. 1999). While in Fig. 4 we show the BATSE spectrum (as re-analysed by us), in the top panel of Fig. 9 we show the *BeppoSAX* data (Frontera et al. 2000). This is because we are here interested in

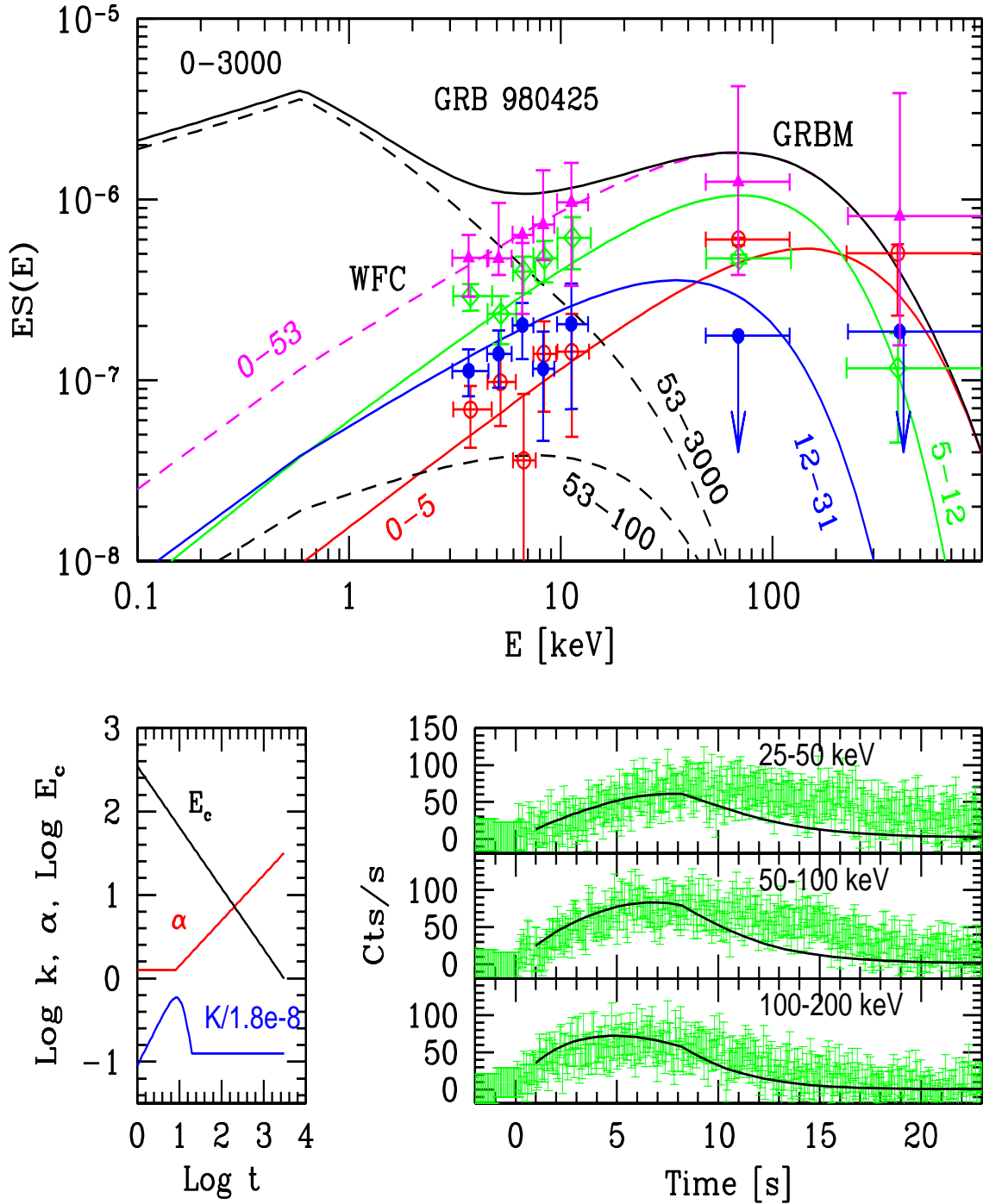


Figure 9. Top panel: the spectral energy distribution of GRB 980425 is compared with the result of our model. Here we show the *BeppoSAX* data, as originally reported by Frontera et al. (2000), in three different time-intervals, and the spectrum time-integrated over the duration of the burst as seen by *BeppoSAX*. The bottom left panel shows how the normalisation $K(t)$, the high energy spectral index α and the cut-off energy E_c change in time. The right bottom panel compares the observed and the calculated light curves in the three labelled energy bands. The observed light curves are from BATSE.

the medium energy X-ray band more than the high energy one. The time integrated fluences of BATSE and the GRBM instrument are consistent. We also show the spectra time-integrated in 3 different time intervals, using the data published in Frontera et al. (2000).

In the right bottom panel of Fig. 9 we show the light curve of the count rate as detected by BATSE, in three

different energy bands [25–50 keV; 50–100 keV and 100–200 keV].

We have then applied our toy model using the same approach described in Sec. 4.2.1. The evolution of $K(t)$, $\alpha(t)$ and $E_c(t)$ is shown in the left bottom panel of Fig. 9.

The resulting spectra are shown as solid lines in the top panel of Fig. 9. They have been time integrated in the

	GRB 980425	GRB 031203	
Observed			
E_{peak}	138	291	keV
E_{iso}	1.62×10^{48}	1.2×10^{49}	erg
Scattering			
E_{peak}	25	30	keV
E_{iso}	9.35×10^{50}	1.93×10^{51}	erg
Spectr. Evo.			
E_{peak}	0.6	5	keV
E_{iso}	2.54×10^{48}	1.6×10^{50}	erg

Table 2. The value of E_{peak} and E_{iso} that are observed and that are predicted by the scattering and spectral evolution models discussed in this paper. These are the values used in Fig 5. Note that the E_{iso} (observed) for GRB 031203 takes into account the small reduction due to the re-analysis of the INTEGRAL data.

same time intervals as the data. We also show the spectrum corresponding to the complete time evolution, assumed to last for 3000 seconds. We have chosen this duration just because it is equal to the one assumed for GRB 031203 and observed for GRB 060218. The calculated light curves are overlapped to the BATSE 64ms observed light curves in the right bottom panel of Fig. 9.

We can see that, again, the calculated spectra and light curves are consistent with what observed. For this burst, unfortunately, we do not have any supplementary information forcing us to believe that the duration of the prompt emission is long (i.e. the WFC was not sensitive enough to follow the burst for a long time, and there was no information about late emission as was the case of the “echo rings” for GRB 031203).

On the other hand, our point is the following: if GRB 980425 is similar to GRB 031203 (and both are similar to GRB 060218), then it is possible that its peak energy E_{peak} is much smaller than what derived by the high energy spectra only. In the case we have just shown $E_{\text{peak}} \sim 0.6$ keV, once the spectrum is integrated over the entire (assumed) duration. Were this the case, then GRB 980425 would not be an outlier any longer, as can be seen in Fig. 5, where we show the new location of this burst.

5 DISCUSSION

In this work we have explored three different scenarios to see if GRB 980425 and GRB 031203 are really outliers with respect to the Amati relation (and therefore also outliers to the Ghirlanda relation) or if they only *appear* as such.

The first model (off axis viewing angle) can bring the two bursts on the Amati relation only if the energetics of these bursts (as would be seen by an on-axis observer) is very large. Such bursts are not expected to exist at low redshifts, and then this argues against this model as an explanation for the two bursts being only “apparent” outliers.

Then we explored the idea that these bursts have “normal” energetics and values of E_{peak} , but both these quantities are modified by a scattering cloud located in the vicinity of the bursts. It must be located in the vicinity of the burst because in this case the prompt emission can completely ionise the material (Lazzati & Perna 2002), making the soft

X-ray afterglow insensitive to absorption. If very close to the burst, the scattering material would be accelerated to large velocities. In the comoving frame of the moving material, incoming photons would be seen redshifted, and a larger fraction of photons would scatter in the Thomson regime. The transmitted spectrum would then be similar (albeit not identical) to the one obtained in the case of a not moving material with a larger τ_T . The complete and exact analysis implies to assume the location and width of the scattering screen, which would determine its acceleration, and this lies outside the aim of this paper.

In this model the intrinsic (i.e. before scattering) energetics is greater than the observed one, but not by a large factor. Even with a substantial value of the scattering optical depth (i.e. $\tau_T \sim \text{a few}$), the reduction in flux of the transmitted radiation is of the order of one–a few hundreds. The scattering process is more effective on low energy X-ray photons, implying that the transmitted spectrum is “bluer” than the intrinsic one. Therefore the intrinsic E_{peak} can be smaller than observed. The two things together (i.e. intrinsically, the two bursts are more energetic and much redder) make it possible for them to lie on the Amati relation. The increase in energetics is not so large to face the problem of having too energetic bursts at small redshifts.

The problem, for this idea, is to explain why these bursts are surrounded by dense and thick material (for scattering), while other bursts are not. The partial answer we can give is to consider one obvious selection effect: we see distant bursts only if they are surrounded by material with a small value of τ_T , since otherwise they go under the detection threshold. Consider that even values of $\tau_T \sim 1$ have almost no effect on the observed spectrum, since in this case more than half of the photons pass through the scattering cloud undisturbed (see Fig. 3). Even the fast variability, if present, would not be smeared out, since the received flux is dominated by the transmitted photons: the scattered ones, having a longer path to travel, arrive later and more diluted in time (i.e. with a much reduced flux).

On the other hand, this model poses several other problems. The most severe of them is that we expect some signature of the presence of such a thick screen in the vicinity of the burst, produced by the collision of the bursts and supernova ejecta with the screen itself.

The third model we have proposed is the most promising, especially after GRB 060218, which we used as a guide to model the two outliers. In this framework the derived intrinsic powers and energetics are the least demanding, as can be seen in Fig. 5 and in Table 2, where we list the values of E_{iso} and E_{peak} for the two bursts. In the framework of this model the presence of both a hard and a soft component (in GRB 031203) is the result of the spectrum evolving in time, and is not due to two separated components (i.e. two emission mechanisms). Note that the real bolometric and time integrated energetics (i.e. E_{iso}) is larger than what derived by considering the high energy spectrum only, but not by a large factor.

The main result of our study is that GRB 031203 and GRB 980425 are likely to be *apparent* outliers: their intrinsic properties are instead consistent with the Amati relation (and therefore it is possible that they obey even the Ghirlanda relation, and they would do so with jet opening angles not particularly extreme, see Fig. 5, although larger

than the average values found for “normal” GRBs). This possibility is strengthened by the fact that GRB 060218, energetically a twin of GRB 031203, lies on the Amati relation independently of our modelling. GRB 980425 and GRB 031203 could also become consistent with the newly found correlation between the peak luminosity of the prompt, E_{peak} and the “high signal” timescale $T_{0.45}$ (Firmani et al. 2006), if they indeed have E_{peak} around ~ 1 keV.

On the other hand these two bursts, together with GRB 060218, besides being underluminous, have a duration much longer than the other bursts, including the X-ray rich and the X-ray flash population of bursts (see e.g. Lamb, Donaghy & Graziani 2005). The inevitable conclusion is that the Amati relation (and possibly the Ghirlanda one) is more robust than previously thought, being obeyed by bursts that are underluminous and with a duration longer than the average one and that (with respect to the Amati relation) GRB 980425 and GRB 031203 are not representative of a different population of objects with respect to “classical” GRBs.

ACKNOWLEDGEMENTS

We thank the Italian INAF for financial support.

REFERENCES

- Amati, L., Frontera, F., Tavani, M. et al., 2002, *A&A*, 390, 81
 Amati, L., 2006, *subm. to MNRAS (astro-ph/0601553)*
 Band, D.L., Norris, J.P. & Bonnell, J.T., 2004, *ApJ*, 613, 484
 Band, D.L., Matteson, J., Ford, L., et al., 1993, *ApJ*, 413, 281
 Band, D.L. & Preece, R.D., 2005, *ApJ*, 627, 319
 Barbiellini, G., Celotti, A., Ghirlanda, G., Longo, F., Piro, L. & Tavani, M., *MNRAS*, 350, L5
 Barthelmy S., Cummings, J., Sakamoto, T., Markwardt, C. & Gehrels, N., 2006, *GCN*, 4806
 Bosnjak, Z., Celotti, A., Longo, F., Barbiellini, G., 2006, *subm. to MNRAS (astro-ph/0502185)*,
 Brainerd, J.J., 1994, *ApJ*, 428, 21
 Brainerd, J.J., Preece, R.D., Briggs, M.S., Pendleton, G.N. & Paciesas, W.S., 1998, *ApJ*, 501, 325
 Cobb, B.E., Bailyn, C.D., van Dokkum, P.G. & Natarajan, P., 2006, *subm. to ApJ (astro-ph/0603832)*
 Campana, S. Mangano, V., Blustin, A.J., et al., 2006, *subm. to Nature (astro-ph-063279)*
 Celotti, A., Maraschi, L., Ghisellini, G., Caccianiga, A. & Maccauro T., 1993, *ApJ*, 416, 118.
 Cusumano, G., Barthelmy, S., Gehrels, N., Hunsberger, S., Immler, S., Marshall, F., Palmer, D., & Sakamoto, T., 2006, *GCN*, 4775
 Dai, Z.G., Zhang, B. & Liang, E.W., 2006, *subm. to ApJ (astro-ph-0604510)*
 Della Valle, M., Malesani, D., Benetti, S. et al., 2003, *A&A*, 406, L33
 Eichler, D. & Levinson, A., 2004, 614, L13
 Firmani, C., Ghisellini, G., Avila-Reese, V. & Ghirlanda, G., 2006, *MNRAS*, in press (astro-ph/0605073)
 Frontera F., Amati L., Costa E. et al. 2000, *ApJS*, 127, 59
 Galama, T., Vreeswijk, P.M., van Paradijs, J., et al., 1998, *Nature*, 395, 678
 Ghirlanda, G., Ghisellini, G. & Lazzati, D., 2004, *ApJ*, 616, 331
 Ghirlanda, G., Celotti A., & Ghisellini, G., 2003, *A&A*, 406, 879
 Ghirlanda, G., Ghisellini, G., Firmani, C., 2005, *MNRAS*, 361, L10
 Ghisellini, G., Celotti, A. & Lazzati, D., 2000, *MNRAS*, 313, L1
 Ghisellini, G. & Lazzati, D., 1999, *MNRAS*, 309, L7
 Greiner, J., Peimbert, M., Estaban, C., et al., 2003, *GCN* 2020
 Guetta, D., Perna, R., Stella, L. & Vietri, M., 2004, *ApJ*, 615, L73
 Lamb, D.Q., Donaghy, T.Q. & Graziani, C., 2005, *ApJ*, 620, 355
 Lazzati, D. & Perna, R., 2002, *MNRAS*, 330, 383
 Liang, E., Zhang, B., Dai, Z.G., 2006, *subm. to ApJ (astro-ph/0605200)*
 Malesani, D., Tagliaferri, G., Chincarini, G., et al., 2004, *ApJ*, 609, L5
 Masetti, N., Palazzi, E., Pian, E. & Patat, F., 2006, *GCN* 4803
 Mirabal, N. & Halpern, J.P., 2006, *GCN* 4792
 Nakar, E. & Piran, T., 2005, *MNRAS*, 360, L73
 Nava, L., Ghisellini, G., Ghirlanda G., Tavecchio, F. & Firmani C., 2006, *A&A*, 450, 471
 Paczynski, B. & Haensel, P., 2005, *MNRAS*, 362, L4
 Pian, E., Amati, L., Antonelli, L.A., et al., 1999, *A&AS*, 138, 463
 Pian, E., Mazzali, P.A., Masetti, N., et al., 2006, *subm. to Nature (astro-ph/0603530)*
 Pian, E., Amati, L., Antonelli, L.A. et al., 2000, *ApJ*, 536, 778
 Preece, R.D., Briggs, M.S., Mallozzi, R.S., Pendleton, G.N., Paciesas, W.S., Band, D.L., 1998, *ApJ*, 506, L23
 Prochaska, J.X., Bloom, J.S., Chen, H., et al., 2004, *ApJ*, 611, 200
 Ramirez-Ruiz, E., Granot, J., Kouveliotou, C., Woosley S.E., Pat-
 tel, S.K. & Mazzali, P., 2005, *ApJ*, 625, L91
 Reichart, D.E., Lamb, D.Q., Fenimore, E.E., Ramirez-Ruiz, E.,
 Cline, T.L. & Hurley, K., 2001, *ApJ*, 552, 57
 Sazonov, S.Y., Lutovinov, A.A., Sunyaev, R.A., 2004, *Nature*,
 430, 646
 Stanek, K.Z., Matheson, T., Garnavich, P.M., et al., *ApJ*, 591,
 L17
 Thomsen, B., Hjorth, J., Watson, D., et al., 2004, *A&A*, 419, L21
 Tiengo, A. & Mereghetti, S., *A&A*, 449, 203
 Tinney, C., Stahakis, R., Cannon, R. & Galama, T.J., 1998, *IAU*
Circ. 6896
 Toma, K., Yamazaki, R. & Nakamura, T., 2005, *ApJ*, 635, 481
 Urry, C.M. & Shafer, R.A., 1984, *ApJ*, 280, 569
 Vaughan, S., Willingale, R., O’Brien, P.T. et al., 2004, *ApJ*, 603,
 L5
 Vaughan, S., Willingale, R., Romano, P., et al., 2006, *ApJ*, 639,
 323
 Vreeswijk, P., Fruchter, A., Hjorth, J. & Kouveliotou, C., 2002,
GCN 1785
 Watson, D., Vaughan, S.A., Willingale, R. et al., 2006, *ApJ*, 636,
 967
 Watson, D., Hiorth, J., Levan, A., et al., 2004, *ApJ*, 605, L101
 Yamazaki, R., Yonetoku, D. & Nakamura, T. 2003, *ApJ*, 594, L79